Chemistry & Biology
Article

Activation State-Dependent Binding of Small Molecule Kinase Inhibitors: Structural Insights from Biochemistry

Lisa M. Wodicka,[1,2] Pietro Ciceri,[1,2] Mindy I. Davis,[1,2] Jeremy P. Hunt,[1] Mark Floyd,[1] Sara Salerno,[1] Xuequn H. Hua,[1] Julia M. Ford,[1] Robert C. Armstrong,[1] Patrick P. Zarrinkar,[1,*] and Daniel K. Treiber[1,*]
[1]Ambit Biosciences, 4215 Sorrento Valley Boulevard, San Diego, CA 92121, USA
[2]These authors contributed equally to this work
*Correspondence: pzarrinkar@ambitbio.com (P.P.Z.), dtreiber@discoverx.com (D.K.T.)
DOI 10.1016/j.chembiol.2010.09.010

SUMMARY

Interactions between kinases and small molecule inhibitors can be activation state dependent. A detailed understanding of inhibitor binding therefore requires characterizing interactions across multiple activation states. We have systematically explored the effects of ABL1 activation loop phosphorylation and PDGFR family autoinhibitory juxtamembrane domain docking on inhibitor binding affinity. For a diverse compound set, the affinity patterns correctly classify inhibitors as having type I or type II binding modes, and we show that juxtamembrane domain docking can have dramatic negative effects on inhibitor affinity. The results have allowed us to associate ligand-induced conformational changes observed in cocrystal structures with specific energetic costs. The approach we describe enables investigation of the complex relationship between kinase activation state and compound binding affinity and should facilitate strategic inhibitor design.

INTRODUCTION

Kinases are dynamic proteins that sample a wide range of conformations, and kinase conformational equilibria are to a large extent governed by the activation state (Huse and Kuriyan, 2002). Binding of small molecule inhibitors can be conformation specific (Schindler et al., 2000), and the nine ATP-competitive kinase inhibitors currently approved for use in humans include nearly equal numbers of molecules that bind to catalytically active and inactive enzyme conformations (Alton and Lunney, 2008). The effects of activation state on small molecule inhibitor binding affinity have largely been inferred from structural observations and are only now beginning to be systematically explored biochemically. To fully characterize the interaction of inhibitors with their targets, it is necessary to quantify the activation state dependence of inhibitor binding, which can have important implications for drug discovery (Alton and Lunney, 2008).

The ABL1-imatinib interaction is perhaps the best understood example of activation state-dependent inhibitor binding. ABL1, like many kinases, is activated in part by activation loop (A-loop) phosphorylation, which stabilizes a catalytically active enzyme conformation (Hantschel et al., 2003; Schindler et al., 2000). Imatinib, however, binds a catalytically inactive conformation of the ABL1 kinase domain (Nagar et al., 2002) that is disfavored in the phosphorylated, activated state. The activation state dependence of imatinib binding has been demonstrated in biochemical studies showing more potent inhibitory activity against nonphosphorylated relative to phosphorylated ABL1 (Seeliger et al., 2007). The second-generation ABL1 inhibitors dasatinib and nilotinib are effective against most imatinib-resistant ABL1 variants (Shah et al., 2004; Weisberg et al., 2005). Nilotinib, like imatinib, is a "type II" inhibitor (Weisberg et al., 2005) defined by a binding mode that features penetration into an "allosteric" binding pocket adjacent to the ATP site, accessible when the A-loop adopts a "DFG-out" inactive conformation (Liu and Gray, 2006), as well as overlap with the ATP site itself. Based upon this conserved binding mode and the available biochemical data, type II inhibitor binding is believed to be sensitive to A-loop phosphorylation (Okram et al., 2006). Conversely, dasatinib is a "type I" inhibitor, defined by a binding mode overlapping the ATP site with no penetration into the allosteric pocket (Tokarski et al., 2006). Type I inhibitors typically do not require a DFG-out conformation for binding, and structural and modeling studies suggest that type I inhibitor binding is compatible with multiple A-loop conformations (Nagar et al., 2002; Tokarski et al., 2006; Vogtherr et al., 2006), including the "DFG-in" active conformation. For this reason, it is believed that type I inhibitor binding is not generally sensitive to A-loop phosphorylation (Okram et al., 2006).

The kinase activation state can also be governed by interactions with regulatory domains. The PDGFR family class III receptor tyrosine kinases (RTKs) CSF1R, FLT3, KIT, and PDGFRα/β, for example, contain a conserved autoinhibitory juxtamembrane (JM) domain that docks with the kinase domain to stabilize a catalytically inactive DFG-out A-loop conformation (Griffith et al., 2004; Mol et al., 2004; Schubert et al., 2007). The JM domain is located between the transmembrane and kinase domains and contains tyrosine phosphorylation sites required for enzyme activation (Hubbard, 2004). The PDGFR family RTKs can exist in at least three distinct activation states (DiNitto et al., 2010): (1) the "autoinhibited," nonphosphorylated state, where the autoinhibited conformation (JM domain docked) predominates; (2) the "nonautoinhibited" state, where the JM domain is phosphorylated and the nonautoinhibited

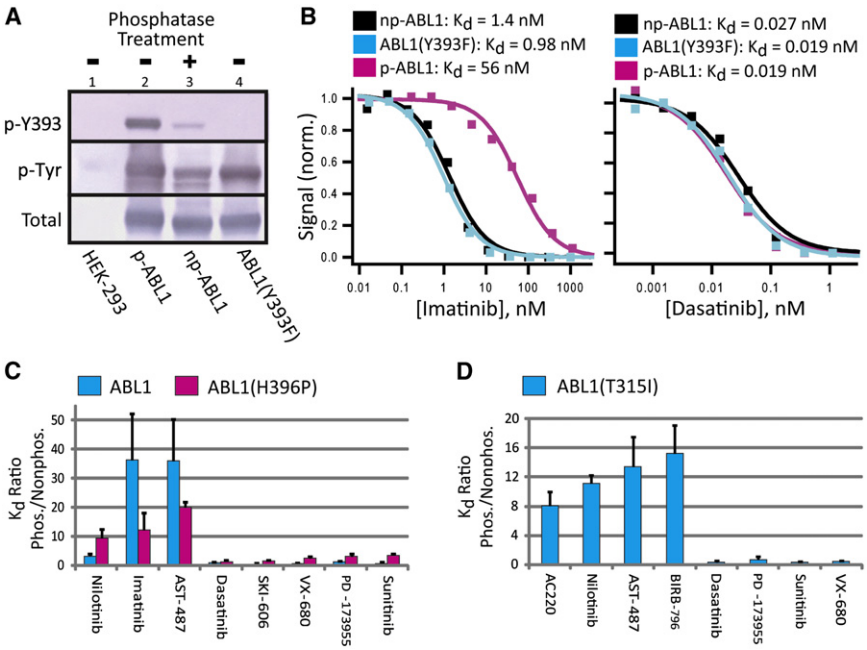

Figure 1. Activation State-Specific ABL1 Assays Functionally Classify Type I and Type II Inhibitors

(A) Western blots comparing A-loop p-Y393 levels (upper) and overall p-Tyr levels (middle) for ABL1 produced with (np-ABL1) or without (p-ABL1) endogenous phosphatase treatment. ABL1 (Y393F) was prepared identically to p-ABL1. Total recombinant ABL1 levels (lower) and results for nontransfected HEK293 cells (lane 1) are indicated.

(B) K_d measurements for the interactions of imatinib and dasatinib with np-ABL1, p-ABL1, and ABL1(Y393F). Assay signals were normalized to facilitate comparison.

(C) For a series of known and predicted type I and type II inhibitors, the phosphorylated (Phos.) to nonphosphorylated (Nonphos.) state K_d ratios are shown for ABL1 and ABL1(H396P). Values >1 indicate preferential affinity for the nonphosphorylated state. Error bars are the standard deviations of the K_d ratios. Individual K_ds are shown in Table S1.

(D) Same as (C), except that K_d ratios are shown for ABL1(T315I). For AC220, the K_d for np-ABL1 (T315I) was 3.7 μM, while the K_d for p-ABL1 (T315I) was above the solubility limit (10 μM) and estimated as 30 μM for the K_d ratio calculation. See Table S2 and Figure S2.

conformation (JM domain not docked) predominates; and (3) the "activated" state, where the nonautoinhibited state is additionally phosphorylated on the A-loop, and the DFG-in conformation is stabilized. Ligand binding to the extracellular domain of the autoinhibited enzyme induces dimerization and *trans*-autophosphorylation of the JM domain, which disrupts interactions with the kinase domain (Mol et al., 2004), effecting a shift to the nonautoinhibited state. The A-loop is subsequently phosphorylated to produce the activated state, which, for KIT, has similar catalytic activity to the nonautoinhibited state (DiNitto et al., 2010). The autoinhibitory function of the JM domain can also be disrupted by mutations, and kinases harboring such activating mutations often drive disease and are targets for kinase inhibitor therapy (Janne et al., 2009). The autoinhibited structures of CSF1R, FLT3, and KIT (Griffith et al., 2004; Mol et al., 2004; Schubert et al., 2007) suggest that JM domain docking is energetically favorable and likely to impact inhibitor binding. Cocrystal structures have revealed a range of inhibitor binding modes that are either largely compatible or incompatible with the autoinhibited conformation (Gajiwala et al., 2009; Mol et al., 2004; Schubert et al., 2007). The structures show that inhibitor binding induces conformational changes relative to the apo-autoinhibited structure, but the associated energetic costs for these changes have not been defined.

Novel binding assays using kinases modified on the A-loop with fluorescent tags have been reported that can identify inhibitors as having DFG-out binding modes, but the effects of activation state on inhibitor binding are just beginning to be explored in this system (Simard et al., 2009). Enzymatic studies on KIT show that A-loop phosphorylation can significantly affect inhibitor potency, but the impact of JM domain docking on inhibitor binding has not been directly addressed (DiNitto et al., 2010). Here, we systematically and quantitatively measure activation state-dependent inhibitor binding affinity in the context of both ABL1 A-loop phosphorylation and JM domain-mediated autoinhibition for class III RTKs.

RESULTS

Inhibitor Binding Assays for ABL1 Differentially Phosphorylated on the A-loop

To systematically measure the effects of ABL1 A-loop phosphorylation on small molecule inhibitor binding affinity, we developed competition binding assays (Karaman et al., 2008). Activation state-specific binding assays do not require catalysis and therefore avoid several problematic aspects of enzyme activity assays, including reduced catalytic activity of the unactivated state, confounding activation of the unactivated state during the assay, and state-dependent K_m(ATP) values. Binding assays may thus provide a more general approach than activity assays to explore activation state-dependent inhibitor binding. The ABL1 kinase domain was expressed in HEK293 cells, and extracts were prepared under conditions that either preserved or greatly reduced A-loop phosphorylation. The A-loop contains a single Tyr residue (Y393), and a western blot with a p-Y393 antibody confirmed that the two kinase preparations had large differences in phosphorylation at this site (Figure 1A, upper, compare lanes 2 and 3). The nonphosphorylatable ABL1 (Y393F) mutant lacked any p-Y393 signal, as expected (lane 4). In contrast, blots probed with a general p-Tyr antibody showed that overall p-Tyr levels were similar for the phosphorylated A-loop (p-ABL1) and ABL1(Y393F) preparations (Figure 1A, middle) and were moderately reduced in the nonphosphorylated A-loop preparation (np-ABL1). Imatinib binding affinity was

dependent on the A-loop phosphorylation state. The binding constants (K_ds) of imatinib for np-ABL1 and ABL1(Y393F) were nearly identical and more than 30-fold lower than the K_d for p-ABL1 (Figure 1B; see Table S1 available online), consistent with the results from enzyme activity assays (Seeliger et al., 2007). In contrast to imatinib, the affinities of the type I inhibitor dasatinib for np-ABL1, ABL1(Y393F), and p-ABL1 were nearly identical (Figure 1B; Table S1). Taken together, these immunoblot and K_d data strongly suggest that the assays specifically query the effects of A-loop phosphorylation on inhibitor binding affinity, though we cannot completely rule out the involvement of p-Tyr residues at other sites.

Distinguishing Type I from Type II Inhibitors

Binding affinity dependent on the phosphorylation state of the ABL1 A-loop may be a general feature of type II inhibitors that offers an approach to functionally classify compounds as type I or type II in the absence of structural information (Okram et al., 2006). To determine how predictive such an approach may be, we measured binding constants for an additional set of known or predicted type I and type II inhibitors for p-ABL1 and np-ABL1 (Table S2). The compounds tested included known ABL1 inhibitors and compounds that are not primarily ABL1 inhibitors, but for which activity against ABL1 has been demonstrated (Carter et al., 2005; Karaman et al., 2008). Nilotinib is a structurally confirmed type II inhibitor (Weisberg et al., 2005), and PD-173955 (Nagar et al., 2002) and VX-680 are structurally confirmed type I inhibitors (Table S2). AST-487 has been hypothesized to be a type II inhibitor based on molecular modeling, and modeling studies also suggest that SKI-606 is a type I inhibitor (Table S2). Sunitinib is an interesting type I inhibitor that has been observed to bind KIT in an autoinhibited, DFG-out conformation but does not penetrate into the allosteric pocket (Gajiwala et al., 2009).

Imatinib and the predicted type II inhibitor AST-487 exhibited a clear preference (>30-fold) for np-ABL1, while nilotinib showed only a small preference (Figure 1C; Table S1). In contrast, the type I inhibitors did not bind preferentially to either form of the kinase (Figure 1C; Table S1). To determine if the relative affinity patterns observed for wild-type ABL1 are retained in an imatinib-resistant mutant variant, we developed assays for ABL1 (H396P) differentially phosphorylated on the A-loop. The results for ABL1(H396P) were similar to wild-type, with the exception that nilotinib was clearly identified as a type II inhibitor, with a 10-fold preference for the nonphosphorylated state (Figure 1C; Table S1). Thus, together the wild-type and H396P mutant assays correctly identify or confirm inhibitor type across this compound set.

To explore how broadly this approach can be applied, we attempted to classify compounds that not only are not primarily ABL1 inhibitors, but that also lack potent binding affinity for wild-type ABL1. We developed assays for the drug-resistant ABL1(T315I) mutant, which binds some inhibitors with higher affinity than wild-type ABL1 (Karaman et al., 2008). BIRB-796 is a confirmed type II p38α inhibitor (Pargellis et al., 2002), while AC220 is a second-generation FLT3 inhibitor with an undefined binding mode (Table S2) (Zarrinkar et al., 2009). AC220 and BIRB-796 have been shown to bind with modest or moderate affinity to ABL1(T315I), respectively, but were poorly detected in wild-type ABL1 assays (Carter et al., 2005; Zarrinkar et al., 2009). Markedly higher affinity was observed for both compounds for np-ABL1(T315I) relative to p-ABL1(T315I) (Figure 1D; Table S1), correctly identifying BIRB-796 as a type II inhibitor, and suggesting that AC220 is a type II inhibitor as well. To determine whether the T315I mutation itself affects the observed binding mode, we tested compounds whose binding affinity relative to wild-type is impacted by this mutation either dramatically (nilotinib, dasatinib, PD-173955), modestly (AST-487), or minimally (VX-680, sunitinib). In all cases, the phosphorylation state dependence of binding affinity was qualitatively the same as for wild-type ABL1 and ABL1(H396P) (Figure 1D; Table S1), and nilotinib was again correctly classified as a type II inhibitor. Thus, the binding mode classifications are consistent across the ABL1 variants tested and are independent of the affinity for a particular ABL1 variant.

These results demonstrate that a suite of activation state-specific ABL1 assays can be used to classify the type I/type II binding mode of inhibitors, including those that primarily target kinases other than ABL1. The consistent trends across multiple ABL1 variants provide added confidence in the classification, as exemplified by nilotinib, where the wild-type ABL1 data alone were equivocal, while data across the full assay suite clearly and correctly identified the type II binding mode. Since the type I/type II inhibitor binding mode is, with rare exceptions (Atwell et al., 2004), generally conserved across kinases (Mol et al., 2004; Namboodiri et al., 2010; Seeliger et al., 2007), we suggest that this approach is informative for a wide range of kinase inhibitors, particularly since ABL1 is a common off-target of compounds that primarily target other kinases (Karaman et al., 2008).

Differential Binding of Both Type I and Type II Inhibitors to Autoinhibited and Nonautoinhibited States of FLT3, KIT, and CSF1R

To measure the effects of JM domain docking on inhibitor affinity for FLT3, KIT, and CSF1R, we developed binding assays for autoinhibited and nonautoinhibited states of each kinase. The JM domain comprises three short motifs, JM-B ("binding"), JM-S ("switch"), and JM-Z ("zipper") (Figure 2A) (Griffith et al., 2004). JM-B closely interacts with multiple key regions of the active site in the autoinhibited conformation, whereas JM-S is a β twist containing tyrosine phosphorylation sites required to switch the enzyme to the nonautoinhibited state, and JM-Z is a linker associated with the N-terminal lobe that positions JM-S and JM-B in the correct register for autoinhibition (Griffith et al., 2004). In a structure of nonautoinhibited KIT di-phosphorylated on JM-S, both JM-B and JM-S are disordered, whereas JM-Z remains ordered and associated with the N-terminal lobe (Mol et al., 2004). To develop assays for the autoinhibited state, we therefore expressed each enzyme with an intact JM domain (JMplus), and to develop assays for the nonautoinhibited state, we expressed truncated proteins lacking JM-B and JM-S, but including JM-Z (JMminus) (Figure 2A). We then measured the binding affinities of several known or predicted type I and type II inhibitors for autoinhibited and nonautoinhibited FLT3, KIT, and CSF1R. For each enzyme, the inhibitor panel included well established inhibitors of the kinase being queried as well as compounds optimized for other kinases that have a broad range of affinities for the queried kinase. Type I inhibitors not tested

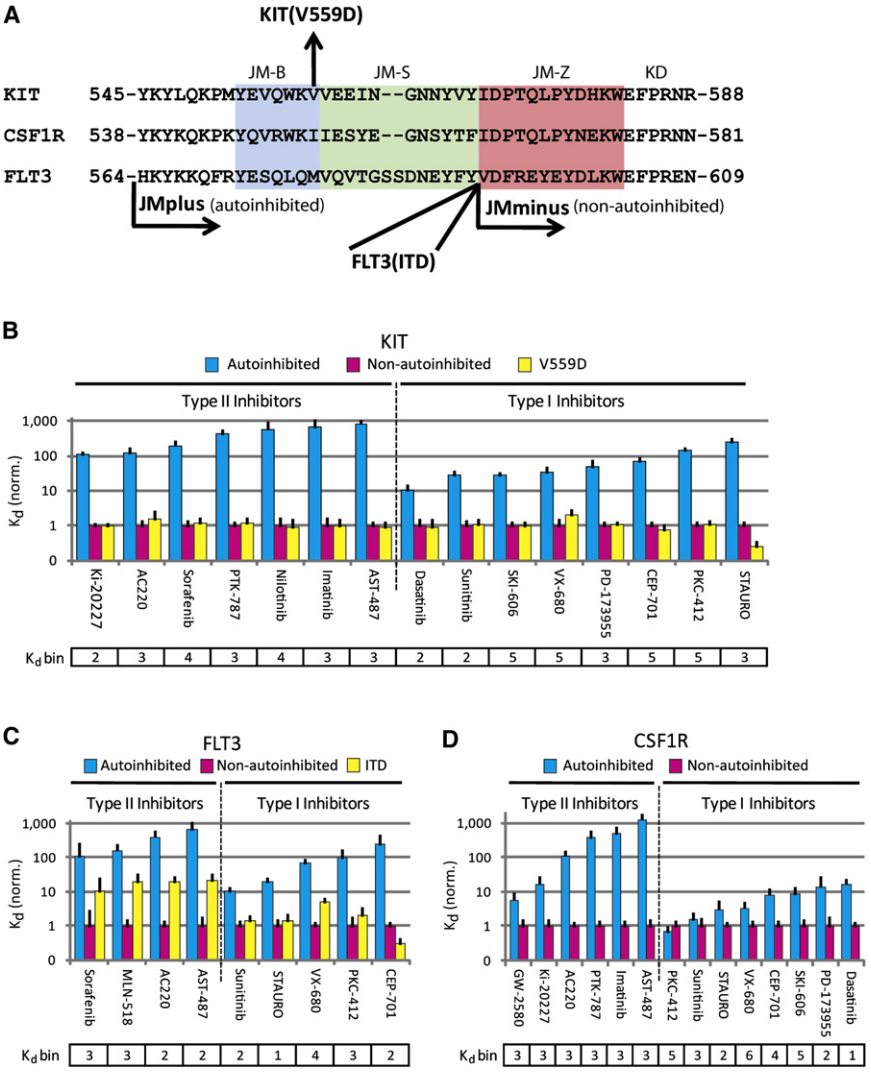

Figure 2. JM Domain Docking Substantially Impacts Inhibitor Binding Affinity for the Class III RTKs KIT, FLT3, and CSF1R

(A) Alignment of the conserved KIT, CSF1R, and FLT3 JM domains showing the constructs used. The N termini of the autoinhibited (JMplus) and nonautoinhibited (JMminus) constructs are indicated, as are the positions of the KIT V559D and FLT3 ITD mutations. Both mutations are in the context of JMplus constructs, and the ITD mutation is described in Supplemental Experimental Procedures. The JM domain submotifs (Griffith et al., 2004) and the start of the kinase domain (KD) are indicated.

(B) Relative binding affinities of known or predicted type I and type II inhibitors for autoinhibited and nonautoinhibited KIT and KIT(V559D). To facilitate visualization of affinity offsets between activation states, the data have been normalized to the K_d values for the nonautoinhibited state. Normalized K_d values of 1 indicate the affinity is equal to that for the nonautoinhibited state, and values >1 indicate a reduced affinity relative to the nonautoinhibited state. K_d values for the nonautoinhibited state spanned several orders of magnitude. To simplify comparison, we assigned each inhibitor to a "K_d bin" based on its affinity for the nonautoinhibited state (shown below chart): bin 1 - K_d = 0.01–0.1 nM; bin 2 - K_d = 0.1–1.0 nM; bin 3 - K_d = 1–10 nM; bin 4 - K_d = 10–100 nM; bin 5 - K_d = 100–1000 nM; bin 6 - K_d = 1000–10,000 nM. Error bars are the standard deviations of the normalized K_ds. Individual K_ds are shown in Table S1.

(C) and (D) Same as (B), except that normalized K_ds are shown for FLT3 and CSF1R assays, respectively. See also Table S2 and Figure S1.

against the ABL1 assays described above included staurosporine (STAUR) and its analogs PKC-412 and CEP-701, and additional known type II inhibitors included the VEGFR2 inhibitor sorafenib and the CSF1R inhibitor GW-2580 (Table S2). Predicted type II inhibitors not tested against the ABL1 assays included the VEGFR2 inhibitor PTK-787, which is related to a known type II inhibitor, as well as Ki-20227 and MLN-518, which have type II-like chemical structures and target CSF1R and FLT3, respectively (Table S2). Inhibitor binding affinity was consistently and in many cases dramatically reduced by JM domain docking for all three RTKs, with most inhibitors having 10- to 1000-fold greater affinity for the nonautoinhibited state relative to the autoinhibited state (Figures 2B–2D; Table S1). These affinity shifts were apparent for both type I and type II inhibitors, unlike for ABL1, where only type II inhibitor affinity was activation state dependent. The magnitude of the affinity shift between nonautoinhibited and autoinhibited states was not dependent on the absolute affinity of compounds for the nonautoinhibited state, with both high affinity and low affinity compounds exhibiting a range of affinity shifts (see "K_d bins" below charts in Figures 2B–2D; Table S1). For KIT and FLT3, type I inhibitors had affinity shifts of 10- to 100-fold, whereas for type II inhibitors the effects were larger (100- to 1000-fold). For CSF1R the affinity shifts for type II inhibitors were more compound dependent, and the two compounds optimized for CSF1R inhibition, GW-2580 and Ki-20227, had only a ≈10-fold preference for the nonautoinhibited state, whereas up to 1000-fold affinity differences were observed for AST-487, imatinib, and PTK-787. Autoinhibited CSF1R was also uniquely tolerant of type I inhibitor binding, with most affinity shifts ≤10-fold, including two compounds, PKC-412 and sunitinib, that did not significantly discriminate between activation states. One explanation for the reduced type I inhibitor affinity shifts for CSF1R is that its docked JM domain may permit more flexibility within the ATP site than the docked KIT and FLT3 JM domains. The overall JM domain docking energies for these kinases may be similar, however, since for all three enzymes, affinity shifts of 1000-fold were observed for imatinib and/or AST-487, which are known or expected to induce undocking of the JM domain upon binding, respectively. These data establish that the activation state for these RTKs can have a large impact on both type I and type II inhibitor affinity, but that some potent inhibitors have similar affinities for both

Table 1. K_d Values for ATP Binding to Autoinhibited, Nonautoinhibited, and Mutant Forms of CSF1R, FLT3, and KIT

Kinase	Activation State	K_d ATP (μM)[a]
CSF1R	Autoinhibited	>1000
	Nonautoinhibited	16 ± 6.1
FLT3	Autoinhibited	>1000
	Nonautoinhibited	7.0 ± 2.3
	ITD	75 ± 22
KIT	Autoinhibited	>1000
	Nonautoinhibited	180 ± 58
	V559D	100 ± 13

See also Figure S1.
[a] Values are the average of at least four measurements ± SD.

states. Interestingly, we did not identify any inhibitors having an affinity preference for the autoinhibited state, and the design of compounds with this profile presents a compelling medicinal chemistry challenge.

Tumorigenic Activating Mutations in the JM Domains of KIT and FLT3 Relieve Autoinhibition to Different Extents

To determine the effect of activating tumorigenic mutations known to interfere with JM domain docking, we also developed assays for FLT3 harboring an internal tandem duplication (ITD), known to be a driver mutation in AML (Meshinchi and Appelbaum, 2009), and for KIT harboring a V559D mutation, known to be a driver mutation in gastrointestinal stromal tumors (Heinrich et al., 2008) (Figure 2A). The activating mutations markedly increased inhibitor binding affinity relative to the autoinhibited state, a result consistent with these mutations disrupting JM domain docking (Figures 2B and 2C; Table S1). The KIT (V559D) data were nearly identical to the nonautoinhibited, JMminus data, suggesting that this mutation is fully penetrant and functionally equivalent to a JM-B/JM-S deletion (Figure 2B). In contrast, the FLT3(ITD) mutation was not fully penetrant, with the type II inhibitors still showing ≈10-fold binding affinity preferences for the nonautoinhibited state (Figure 2C; Table S1). The particular ITD used in our constructs is an insertion between the JM-Z and JM-S motifs that is likely to have unfavorable entropic consequences for JM domain docking, but unlikely to directly disrupt JM-B and JM-S (Figure 2A), which could explain the lack of full penetrance. Conversely, the KIT V559D mutation is within the critical JM-B motif and likely disrupts docking directly (Figure 2A). Thus, these data also provide information about protein structure and stability, where the inhibitors probe the energetic consequences of activating mutations.

ATP Binding Affinity is Activation State Dependent for KIT, FLT3, and CSF1R

ATP binding affinity is a key parameter that governs the effective cellular potency of ATP-competitive small molecule kinase inhibitors. To determine the activation state dependence of ATP binding, we measured ATP affinity for each of the autoinhibited, nonautoinhibited and mutant enzyme forms. No binding was detected at 1 mM ATP for any of the autoinhibited states, while the K_d for ATP was in the 10–200 μM range for the nonautoinhibited states (Table 1). As was observed for inhibitor binding, the KIT(V559D) mutant behaved identically to the nonautoinhibited state, and the FLT3(ITD) mutant had an intermediate affinity, consistent with full and partial release of autoinhibition for these mutants, respectively. The autoinhibited state is thus not anticipated to significantly bind ATP at physiological concentrations, which makes it an attractive target for ATP-competitive inhibitors.

Further Characterization and Validation of the Activation State-Specific RTK Inhibitor Binding Assays

During this study we further characterized and validated the autoinhibited, nonautoinhibited, and mutant RTK assays in three ways. First, to ensure that any low level of autophosphorylation occurring during protein expression was not a confounding factor, we also tested kinase preparations made by treating the HEK293 cells with potent inhibitors during protein expression, which reduced p-Tyr levels by ≥80% (see Supplemental Experimental Procedures). For all but one assay, nearly identical compound binding affinity data were measured for kinases prepared in the presence or absence of inhibitor, demonstrating that the autoinhibited assays query the fully autoinhibited state and that any low level of JM domain or A-loop phosphorylation was not impacting the results for the nonautoinhibited and mutant assays (Table S1). These results confirm that the assays exclusively address the effects of JM docking on inhibitor binding and not the effects of downstream A-loop phosphorylation. The lone exception was the autoinhibited CSF1R assay, where the K_d values for some type II inhibitors were marginally increased for the inhibitor-treated preparation relative to the standard preparation (Table S1). For this reason, the autoinhibited CSF1R data described above were all measured for the inhibitor-treated enzyme preparation, ensuring that the fully autoinhibited state was queried. Second, to further confirm that the JMminus constructs were an appropriate surrogate for the nonautoinhibited state, we measured cellular IC_{50}s for several inhibitors against ligand-stimulated KIT. Across nine inhibitors, the nonautoinhibited K_d and cellular IC_{50} rank orders were nearly identical, with imatinib being the lone exception (Figure S1). The nonautoinhibited K_ds were generally about 10-fold lower than the cellular IC_{50}s, an offset likely due to competition with ATP in the cellular milieu (Table 1). In contrast, the autoinhibited K_d values were generally ≥10-fold higher than the cellular IC_{50} values, consistent with the nonautoinhibited state being queried in the ligand-stimulated cellular assay. Third, we tested imatinib, sunitinib, and dasatinib in KIT enzyme activity assays performed by three commercial vendors. KIT constructs including the JM domain were used for these assays, and in all cases the in vitro IC_{50} values were ≥10-fold higher than the cellular IC_{50} values, and closer to the autoinhibited state K_ds than to the nonautoinhibited state K_ds (Figure S1). These data suggest that the enzyme preparations were at least partially autoinhibited. In support of this hypothesis, additional tests in a commercial assay for KIT harboring an activating JM domain mutation (V560G) yielded IC_{50} values for all three inhibitors that were ≥100-fold lower than the values measured for wild-type KIT (data not shown). Overall, these results support the use of JMminus constructs as surrogates for the nonautoinhibited state, and both our results and results from others (DiNitto et al., 2010) suggest that in vitro enzyme activity data for these

RTKs should be interpreted carefully, particularly when the activation state is not clearly defined.

DISCUSSION

ABL1 Activation State-Dependent Binding Functionally Classifies Inhibitor Binding Mode

Determining ABL1 activation state-specific binding affinity can classify inhibitors as having type I or type II binding modes in the absence of cocrystal structures. Importantly, correct classifications are made for inhibitors that primarily target kinases other than ABL1, suggesting that this approach would be of general utility in kinase inhibitor discovery. This albeit low resolution structural classification is relevant since important drug-like properties of kinase inhibitors are likely affected by this parameter, including kinome selectivity (Schindler et al., 2000), target residence time (Pargellis et al., 2002), and affinity for enzyme conformations relevant to specific disease indications (Gajiwala et al., 2009; Shah et al., 2004). It is thus likely that the optimal binding mode shall be both kinase and indication specific. For example, type I inhibitors can have clear advantages over type II inhibitors in diseases driven by kinases that harbor activating and resistance mutations that significantly stabilize the enzyme's active conformation (DiNitto et al., 2010; Gajiwala et al., 2009; Shah et al., 2002, 2004). Since the optimal inhibitor binding mode is often unknown at the outset of a discovery program, it can be helpful to identify a set of lead compounds that includes both type I and type II inhibitors. A data-driven determination of the ideal inhibitor type can then proceed during lead optimization, based on performance in downstream assays. Activation state-specific assays should facilitate this strategic approach, particularly in the context of high-throughput, multikinase profiling initiatives across multiple chemical series (Goldstein et al., 2008).

The Energetic Consequences of ABL1 A-loop Phosphorylation on Type I and Type II Inhibitor Binding

While type II inhibitors exhibited a consistent preference for the nonphosphorylated state of ABL1, the effect of phosphorylation was generally moderate (10- to 30-fold). These data suggest that sampling of the DFG-out A-loop conformation is not dramatically reduced upon activation, which highlights the important distinction between activation state and conformational state, since activated enzymes nevertheless sample inactive conformations. There are few examples apart from the ABL1-imatinib interaction where the effects of A-loop phosphorylation on inhibitor binding have been systematically addressed (Hantschel et al., 2003; Seeliger et al., 2007), but the effects are likely to be kinase specific. For example, while inhibitor binding to KIT was dramatically affected by A-loop phosphorylation (DiNitto et al., 2010), no effects on type II inhibitor binding were observed for p38α (Sullivan et al., 2005). None of the type I inhibitors exhibited a significant activation state preference (Figures 1C and 1D; Table S1), and there are at least two possible explanations for this result. One explanation is that type I inhibitors are tolerant of conformational variability and bind equally well to multiple active-like and inactive conformations (Figure S2C) (Nagar et al., 2002; Shah et al., 2004; Tokarski et al., 2006; Vogtherr et al., 2006). This hypothesis would require that all of the type I inhibitors are equally tolerant of conformational variability, which, given the chemical diversity within this set (Table S2), would seem unlikely. A nonmutually exclusive explanation is that, even for the nonphosphorylated state, ABL1 exists primarily in an active-like conformation, a hypothesis consistent with the high catalytic activity of the nonphosphorylated ABL1 kinase domain (Schindler et al., 2000). For this thermodynamic model, the apparent K_d values for type I inhibitor binding are independent of the phosphorylation state, regardless of the tolerance for conformational variability (Figure S2B). NMR studies have shown that dasatinib binds an active-like conformation of nonphosphorylated ABL1 (Vajpai et al., 2008) and suggest that a DFG-in A-loop conformation may be obligatory for binding, which would predict an enhanced affinity for p-ABL1 relative to np-ABL1. We observe, however, that dasatinib binding affinity is not activation state dependent (Figures 1B–1D; Table S1), which may suggest that both ABL1 activation states primarily sample active-like conformations, as discussed above (Figure S2B). Additional structural studies on apo-ABL1 are required to further define the A-loop conformation(s) required for dasatinib binding, and we emphasize that activation state-independent binding does not necessarily prove a lack of conformation-specific binding. In contrast to dasatinib, sunitinib is a type I inhibitor shown to have an apparent obligatory DFG-out binding mode for autoinhibited KIT (Gajiwala et al., 2009) and would thus be expected to have an affinity preference for np-ABL1 similar to type II inhibitors (Figure S2A). We show, however, that sunitinib binding is not activation state dependent (Figures 1C and 1D; Table S1). One possible explanation for this disconnect is that sunitinib has different binding modes for ABL1 and KIT, with only KIT requiring the DFG-out A-loop conformation. In support of this hypothesis, cocrystal structures of inhibitors related to sunitinib bound to FGFR1 reveal a DFG-in binding mode (Mohammadi et al., 1997).

Activation State-Dependent Binding Affinity Measures the Degree of Conformational Change Induced by Inhibitor Binding to Autoinhibited Class III RTKs

In the autoinhibited state, the docked JM domain can interfere with inhibitor binding in two ways: first, by sterically clashing with the inhibitor directly, and, second, by stabilizing an enzyme conformation incompatible with inhibitor binding. Relative affinity preferences for the nonautoinhibited state likely reflect the degree to which the autoinhibited conformation must be disrupted to accommodate inhibitor binding. A crystal structure of imatinib bound to KIT (PDB ID 1T46) (Mol et al., 2004) has shown that binding is sterically incompatible with docking of the JM domain, whereas a crystal structure of sunitinib bound to KIT has revealed a binding mode compatible with a docked JM domain (PDB ID 3G0E) (Gajiwala et al., 2009). These structures are consistent with the much larger affinity preferences for the nonautoinhibited state observed here for imatinib compared with sunitinib. Similarly, a crystal structure of the type II inhibitor GW-2580 bound to autoinhibited CSF1R shows only minor conformational changes relative to the apo-autoinhibited structure (Shewchuk et al., 2004), consistent with the relatively small affinity preference for the nonautoinhibited state measured here. In some cases, type I inhibitors, which should not sterically clash with a docked JM domain, nevertheless are

nearly as disruptive to the autoinhibited conformation as many type II inhibitors, likely due to a requirement for rearrangements of the DFG triad and the P loop, which are held in position by the JM domain (Griffith et al., 2004). Indeed, cocrystal structures of type I inhibitors bound to autoinhibited CSF1R show a range of conformational changes in the binding site relative to the apo-structure, yet the JM domain remains docked (Huang et al., 2008, 2009; Schubert et al., 2007). Interestingly, a recent crystal structure has shown that binding of a type I inhibitor can induce undocking of the JM domain, presumably by forcing the A-loop into a DFG-in conformation (Meyers et al., 2010). Thus, inhibitor binding may also potentially undock the JM domain by an allosteric mechanism, even in the absence of direct steric clashes. Large affinity preferences for the nonautoinhibited state, similar to imatinib, would be predicted for inhibitors acting through this mechanism.

A recent model for KIT activation based on enzyme activity data proposes that the autoinhibited state is sensitive to imatinib (DiNitto et al., 2010), which is inconsistent with the results shown here. One explanation for this apparent discrepancy may be the difficulty of directly querying the low activity, autoinhibited state with enzyme activity assays. Our results do support the hypothesis that dasatinib binding is conformationally tolerant (Tokarski et al., 2006), since only a small preference for the nonautoinhibited state was measured. If dasatinib binding strictly required a DFG-in A-loop conformation, a much larger preference would be expected. The data therefore suggest that dasatinib binding is largely compatible with the DFG-out A-loop conformation that predominates in the autoinhibited state.

When combined with structural data, these biochemical data can estimate the energetic ''price tags'' for specific perturbations to the apo-autoinhibited structure that are induced upon inhibitor binding. This may be valuable for structure-guided drug design and for molecular modeling in general. Even in the absence of crystal structures, activation state-specific binding data can provide structure-function information that characterizes both type I and type II inhibitors based on their compatibility with the autoinhibited conformation. In principle, the data could be used during lead optimization to monitor the impact of chemical changes on detailed inhibitor binding mode. Since PDGFR family kinases are commonly observed off-targets (Karaman et al., 2008), the approach should also be useful for characterizing inhibitors primarily targeting kinases from other classes.

The energetic penalties associated with conformational changes to the autoinhibited structure are surprisingly large. The ≈1000-fold affinity preference of imatinib for the nonautoinhibited state suggests that undocking of the JM domain has a cost of ≈3.5 kcal/mol. Even minor perturbations to the autoinhibited conformation can have a significant energetic cost. For example, sunitinib is known to induce only a minor repositioning of the DFG triad upon binding to autoinhibited KIT (Gajiwala et al., 2009), but nonetheless has a 30-fold affinity preference for the nonautoinhibited state. These findings illustrate how biochemical data can be used to interpret structural data, which do not provide quantitative thermodynamic information. Furthermore, the results differentiate JM domain mutations based on their relative ability to relieve autoinhibition, suggesting that the structural consequences of activating mutations can be inferred from these types of data.

Activation State-Dependent Inhibitor Binding to PDGFR Family RTKs: Implications for Drug Discovery

Small molecule kinase inhibitors should ideally target the disease-driving activation state and any additional states known to be induced by acquired resistance mutations. For diseases driven by kinases harboring JM domain mutations, the nonautoinhibited state is the relevant target initially, but second site A-loop mutations can emerge during treatment that confer inhibitor resistance by effecting a shift to the activated state (DiNitto et al., 2010; Gajiwala et al., 2009). Next-generation inhibitors should therefore target both the nonautoinhibited and activated states, in contrast to imatinib and sunitinib, which lack potency against the activated state (DiNitto et al., 2010). For diseases driven by mutant kinases, the autoinhibited state is less relevant and should be avoided to minimize any undesired effects on normal cells. Conversely, for diseases driven by a wild-type enzyme, the autoinhibited state may be an attractive target for novel inhibitor discovery: this state lacks significant ATP affinity, which should enhance cellular inhibitor potency; and the docked JM domain may provide additional diversity within the binding site, facilitating the design of inhibitors having novel and selective inhibition profiles.

SIGNIFICANCE

Kinases exist in multiple activation states that govern the enzymes' conformational ensemble, and small molecule binding can be activation state dependent. The effects of activation state on inhibitor binding, however, are just beginning to be explored systematically. Here, for two very different modes of activation, we have quantitatively and systematically measured the effects of activation state on inhibitor binding affinity. Results from phosphorylation state-specific binding assays for ABL1 have shown that type II, but not type I, inhibitor binding is activation state dependent, and that the assays can be used to correctly classify compounds as having type I or type II binding modes. Though an inhibitor's binding mode affects several properties relevant for drugs, it is often not characterized due to the requirement for cocrystal structures. The biochemical approach we describe removes this bottleneck and should be of great utility in kinase inhibitor discovery. In a second system exploring the impact of autoinhibitory JM domain docking on inhibitor binding to PDGFR family RTKs, a range of effects on binding affinity were observed for both type I and type II inhibitors. Cocrystal structures have shown that inhibitor binding induces perturbations to the autoinhibited conformation ranging in severity from minor rearrangements of the A-loop to complete undocking of the JM domain. The energetic costs for these induced conformational perturbations have not previously been defined, and the binding results show that these costs scale with the severity of the induced perturbation. For inhibitors like imatinib, which induce complete undocking of the JM domain, the costs can be quite large (≈3.5 kcal/mol). The approach we describe should facilitate structure-guided drug design and also the strategic optimization of inhibitors best suited for specific disease indications.

EXPERIMENTAL PROCEDURES

Inhibitors and Antibodies

See Supplemental Experimental Procedures.

Protein Expression

All enzyme constructs were expressed as N-terminal fusions to the DNA binding domain of NFκB in transiently transfected HEK293 cells. Detailed construct information is provided in Supplemental Experimental Procedures. For the autoinhibited CSF1R construct, transfected cells were treated with 500 nM dasatinib for 1 hr prior to harvest to inhibit activating autophosphorylation. Cell extracts were prepared in M-PER extraction buffer (Pierce) in the presence of Protease Inhibitor Cocktail Complete (Roche) and Phosphatase Inhibitor Cocktail Set II (Merck) per manufacturers' instructions. Phosphatase inhibitors were omitted for the np-ABL1, np-ABL1(H396P), and autoinhibited CSF1R preparations. For p-ABL1, ABL1(Y393F), p-ABL1 (H396P), and p-ABL1(T315I), phosphatase inhibitors were added 2 hr prior to cell harvest to further preserve phosphorylation. For np-ABL1 and np-ABL1(H396P), extracts were incubated for 45 min at 30°C, allowing endogenous phosphatases to dephosphorylate p-Y393. For np-ABL1 (T315I) the construct contained a Y393F mutation to prevent phosphorylation at this site.

Competition Binding Assays

Inhibitor binding constants were measured by using active site-dependent competition binding assays essentially as described (Karaman et al., 2008). In brief, kinases were labeled with a chimeric double-stranded DNA tag containing the NFκB binding site (5′-GGGAATTCCC-3′) fused to an amplicon for qPCR readout, which was added directly to the expression extracts. Binding reactions were assembled by combining DNA-tagged kinase extract, affinity beads loaded with a kinase inhibitor probe molecule (see Supplemental Experimental Procedures), and test compound in 1× binding buffer (PBS/0.05% Tween 20/10 mM DTT/0.1% BSA/2 μg/ml sonicated salmon sperm DNA). Extracts were used directly in binding assays without any enzyme purification steps at a ≥10,000-fold overall stock dilution (final DNA-tagged enzyme concentration <0.1 nM). Assays were incubated for 1 hr at room temperature, which was sufficient to establish equilibrium. $MgCl_2$ (2 mM) was included in all ATP binding studies. Subsequent washing, elution, and qPCR readout steps were as described (Karaman et al., 2008). For each assay the affinity probe concentrations were optimized to ensure that true thermodynamic inhibitor K_d values were measured, as described in Supplemental Experimental Procedures.

Error Analysis

All reported K_d values are the average of at least four measurements made in at least two separate experiments. Standard deviations are reported in Table S1, and coefficients of variation were generally ≈20%. For K_d ratios (Figure 1) and normalized K_ds (Figure 2), propagated errors for quotients were calculated by using the equation:

$$(X1 \pm S1)/(X2 \pm S2) = (X1/X2) \pm (X1/X2)\left((S1/X1)^2 + (S2/X2)^2\right)^{0.5},$$

where X and S are averages and standard deviations, respectively.

SUPPLEMENTAL INFORMATION

Supplemental Information includes Supplemental Experimental Procedures, two figures, and two tables and can be found with this article online at doi:10.1016/j.chembiol.2010.09.010.

ACKNOWLEDGMENTS

We thank Raffaella Faraoni, Michael Hocker, and Warren Lewis for compound synthesis and Lisa Ramos for expert technical assistance. Wendell Wierenga is thanked for critically reading the manuscript and for helpful discussions. All authors are current or former employees of Ambit Biosciences.

Received: July 2, 2010
Revised: August 25, 2010
Accepted: September 14, 2010
Published: November 23, 2010

REFERENCES

Alton, G., and Lunney, E. (2008). Targeting the unactivated conformations of protein kinases for small molecule drug discovery. Expert Opin. Drug Discov. *3*, 595–603.

Atwell, S., Adams, J.M., Badger, J., Buchanan, M.D., Feil, I.K., Froning, K.J., Gao, X., Hendle, J., Keegan, K., Leon, B.C., et al. (2004). A novel mode of Gleevec binding is revealed by the structure of spleen tyrosine kinase. J. Biol. Chem. *279*, 55827–55832.

Carter, T.A., Wodicka, L.M., Shah, N.P., Velasco, A.M., Fabian, M.A., Treiber, D.K., Milanov, Z.V., Atteridge, C.E., Biggs, W.H., 3rd, Edeen, P.T., et al. (2005). Inhibition of drug-resistant mutants of ABL, KIT, and EGF receptor kinases. Proc. Natl. Acad. Sci. USA *102*, 11011–11016.

DiNitto, J.P., Deshmukh, G.D., Zhang, Y., Jacques, S.L., Coli, R., Worrall, J.W., Diehl, W., English, J.M., and Wu, J.C. (2010). Function of activation loop tyrosine phosphorylation in the mechanism of c-Kit auto-activation and its implication in sunitinib resistance. J. Biochem. *147*, 601–609.

Gajiwala, K.S., Wu, J.C., Christensen, J., Deshmukh, G.D., Diehl, W., DiNitto, J.P., English, J.M., Greig, M.J., He, Y.A., Jacques, S.L., et al. (2009). KIT kinase mutants show unique mechanisms of drug resistance to imatinib and sunitinib in gastrointestinal stromal tumor patients. Proc. Natl. Acad. Sci. USA *106*, 1542–1547.

Goldstein, D.M., Gray, N.S., and Zarrinkar, P.P. (2008). High-throughput kinase profiling as a platform for drug discovery. Nat. Rev. Drug Discov. *7*, 391–397.

Griffith, J., Black, J., Faerman, C., Swenson, L., Wynn, M., Lu, F., Lippke, J., and Saxena, K. (2004). The structural basis for autoinhibition of FLT3 by the juxtamembrane domain. Mol. Cell *13*, 169–178.

Hantschel, O., Nagar, B., Guettler, S., Kretzschmar, J., Dorey, K., Kuriyan, J., and Superti-Furga, G. (2003). A myristoyl/phosphotyrosine switch regulates c-Abl. Cell *112*, 845–857.

Heinrich, M.C., Owzar, K., Corless, C.L., Hollis, D., Borden, E.C., Fletcher, C.D., Ryan, C.W., von Mehren, M., Blanke, C.D., Rankin, C., et al. (2008). Correlation of kinase genotype and clinical outcome in the North American Intergroup Phase III Trial of imatinib mesylate for treatment of advanced gastrointestinal stromal tumor: CALGB 150105 Study by Cancer and Leukemia Group B and Southwest Oncology Group. J. Clin. Oncol. *26*, 5360–5367.

Huang, H., Hutta, D.A., Hu, H., DesJarlais, R.L., Schubert, C., Petrounia, I.P., Chaikin, M.A., Manthey, C.L., and Player, M.R. (2008). Design and synthesis of a pyrido[2,3-d]pyrimidin-5-one class of anti-inflammatory FMS inhibitors. Bioorg. Med. Chem. Lett. *18*, 2355–2361.

Huang, H., Hutta, D.A., Rinker, J.M., Hu, H., Parsons, W.H., Schubert, C., DesJarlais, R.L., Crysler, C.S., Chaikin, M.A., Donatelli, R.R., et al. (2009). Pyrido[2,3-d]pyrimidin-5-ones: a novel class of antiinflammatory macrophage colony-stimulating factor-1 receptor inhibitors. J. Med. Chem. *52*, 1081–1099.

Hubbard, S.R. (2004). Juxtamembrane autoinhibition in receptor tyrosine kinases. Nat. Rev. Mol. Cell Biol. *5*, 464–471.

Huse, M., and Kuriyan, J. (2002). The conformational plasticity of protein kinases. Cell *109*, 275–282.

Janne, P.A., Gray, N., and Settleman, J. (2009). Factors underlying sensitivity of cancers to small-molecule kinase inhibitors. Nat. Rev. Drug Discov. *8*, 709–723.

Karaman, M.W., Herrgard, S., Treiber, D.K., Gallant, P., Atteridge, C.E., Campbell, B.T., Chan, K.W., Ciceri, P., Davis, M.I., Edeen, P.T., et al. (2008). A quantitative analysis of kinase inhibitor selectivity. Nat. Biotechnol. *26*, 127–132.

Liu, Y., and Gray, N.S. (2006). Rational design of inhibitors that bind to inactive kinase conformations. Nat. Chem. Biol. *2*, 358–364.

Meshinchi, S., and Appelbaum, F.R. (2009). Structural and functional alterations of FLT3 in acute myeloid leukemia. Clin. Cancer Res. *15*, 4263–4269.

Meyers, M.J., Pelc, M., Kamtekar, S., Day, J., Poda, G.I., Hall, M.K., Michener, M.L., Reitz, B.A., Mathis, K.J., Pierce, B.S., et al. (2010). Structure-based drug design enables conversion of a DFG-in binding CSF-1R kinase inhibitor to a DFG-out binding mode. Bioorg. Med. Chem. Lett. *20*, 1543–1547.

Mohammadi, M., McMahon, G., Sun, L., Tang, C., Hirth, P., Yeh, B.K., Hubbard, S.R., and Schlessinger, J. (1997). Structures of the tyrosine kinase domain of fibroblast growth factor receptor in complex with inhibitors. Science *276*, 955–960.

Mol, C.D., Dougan, D.R., Schneider, T.R., Skene, R.J., Kraus, M.L., Scheibe, D.N., Snell, G.P., Zou, H., Sang, B.C., and Wilson, K.P. (2004). Structural basis for the autoinhibition and STI-571 inhibition of c-Kit tyrosine kinase. J. Biol. Chem. *279*, 31655–31663.

Nagar, B., Bornmann, W.G., Pellicena, P., Schindler, T., Veach, D.R., Miller, W.T., Clarkson, B., and Kuriyan, J. (2002). Crystal structures of the kinase domain of c-Abl in complex with the small molecule inhibitors PD173955 and imatinib (STI-571). Cancer Res. *62*, 4236–4243.

Namboodiri, H.V., Bukhtiyarova, M., Ramcharan, J., Karpusas, M., Lee, Y., and Springman, E.B. (2010). Analysis of imatinib and sorafenib binding to p38alpha compared with c-Abl and b-Raf provides structural insights for understanding the selectivity of inhibitors targeting the DFG-out form of protein kinases. Biochemistry *49*, 3611–3618.

Okram, B., Nagle, A., Adrian, F.J., Lee, C., Ren, P., Wang, X., Sim, T., Xie, Y., Wang, X., Xia, G., et al. (2006). A general strategy for creating ''inactive-conformation'' abl inhibitors. Chem. Biol. *13*, 779–786.

Pargellis, C., Tong, L., Churchill, L., Cirillo, P.F., Gilmore, T., Graham, A.G., Grob, P.M., Hickey, E.R., Moss, N., Pav, S., et al. (2002). Inhibition of p38 MAP kinase by utilizing a novel allosteric binding site. Nat. Struct. Biol. *9*, 268–272.

Schindler, T., Bornmann, W., Pellicena, P., Miller, W.T., Clarkson, B., and Kuriyan, J. (2000). Structural mechanism for STI-571 inhibition of abelson tyrosine kinase. Science *289*, 1938–1942.

Schubert, C., Schalk-Hihi, C., Struble, G.T., Ma, H.C., Petrounia, I.P., Brandt, B., Deckman, I.C., Patch, R.J., Player, M.R., Spurlino, J.C., et al. (2007). Crystal structure of the tyrosine kinase domain of colony-stimulating factor-1 receptor (cFMS) in complex with two inhibitors. J. Biol. Chem. *282*, 4094–4101.

Seeliger, M.A., Nagar, B., Frank, F., Cao, X., Henderson, M.N., and Kuriyan, J. (2007). c-Src binds to the cancer drug imatinib with an inactive Abl/c-Kit conformation and a distributed thermodynamic penalty. Structure *15*, 299–311.

Shah, N.P., Nicoll, J.M., Nagar, B., Gorre, M.E., Paquette, R.L., Kuriyan, J., and Sawyers, C.L. (2002). Multiple BCR-ABL kinase domain mutations confer polyclonal resistance to the tyrosine kinase inhibitor imatinib (STI571) in chronic phase and blast crisis chronic myeloid leukemia. Cancer Cell *2*, 117–125.

Shah, N.P., Tran, C., Lee, F.Y., Chen, P., Norris, D., and Sawyers, C.L. (2004). Overriding imatinib resistance with a novel ABL kinase inhibitor. Science *305*, 399–401.

Shewchuk, L.M., Hassell, A.M., Holmes, D.W., Veal, J.M., Emmerson, H.K., Musso, D.L., Chamberlain, S.D., and Peckham, G.E. (2004). Crystal structure of liganded CFMS kinase domain. US 2004/0002145 A1.

Simard, J.R., Grutter, C., Pawar, V., Aust, B., Wolf, A., Rabiller, M., Wulfert, S., Robubi, A., Kluter, S., Ottmann, C., et al. (2009). High-throughput screening to identify inhibitors which stabilize inactive kinase conformations in p38alpha. J. Am. Chem. Soc. *131*, 18478–18488.

Sullivan, J.E., Holdgate, G.A., Campbell, D., Timms, D., Gerhardt, S., Breed, J., Breeze, A.L., Bermingham, A., Pauptit, R.A., Norman, R.A., et al. (2005). Prevention of MKK6-dependent activation by binding to p38alpha MAP kinase. Biochemistry *44*, 16475–16490.

Tokarski, J.S., Newitt, J.A., Chang, C.Y., Cheng, J.D., Wittekind, M., Kiefer, S.E., Kish, K., Lee, F.Y., Borzillerri, R., Lombardo, L.J., et al. (2006). The structure of Dasatinib (BMS-354825) bound to activated ABL kinase domain elucidates its inhibitory activity against imatinib-resistant ABL mutants. Cancer Res. *66*, 5790–5797.

Vajpai, N., Strauss, A., Fendrich, G., Cowan-Jacob, S.W., Manley, P.W., Grzesiek, S., and Jahnke, W. (2008). Solution conformations and dynamics of ABL kinase-inhibitor complexes determined by NMR substantiate the different binding modes of imatinib/nilotinib and dasatinib. J. Biol. Chem. *283*, 18292–18302.

Vogtherr, M., Saxena, K., Hoelder, S., Grimme, S., Betz, M., Schieborr, U., Pescatore, B., Robin, M., Delarbre, L., Langer, T., et al. (2006). NMR characterization of kinase p38 dynamics in free and ligand-bound forms. Angew. Chem. Int. Ed. Engl. *45*, 993–997.

Weisberg, E., Manley, P.W., Breitenstein, W., Bruggen, J., Cowan-Jacob, S.W., Ray, A., Huntly, B., Fabbro, D., Fendrich, G., Hall-Meyers, E., et al. (2005). Characterization of AMN107, a selective inhibitor of native and mutant Bcr-Abl. Cancer Cell *7*, 129–141.

Zarrinkar, P.P., Gunawardane, R.N., Cramer, M.D., Gardner, M.F., Brigham, D., Belli, B., Karaman, M.W., Pratz, K.W., Pallares, G., Chao, Q., et al. (2009). AC220 is a uniquely potent and selective inhibitor of FLT3 for the treatment of acute myeloid leukemia (AML). Blood *114*, 2984–2992.